William R. Dickinson, Richard A. Armin, Nancy Beckvar, Thomas C. Goodlin, Susanne U. Janecke, Roger A. Mark, Richard D. Norris, Gregg Radel, and Ann A. Wortman

Laboratory of Geotectonics, Department of Geosciences
University of Arizona, Tucson, Arizona 85721

1

GEOHISTORY ANALYSIS OF RATES OF SEDIMENT ACCUMULATION AND SUBSIDENCE FOR SELECTED CALIFORNIA BASINS

Geohistory analysis of basin subsidence affords important insights into the tectonic history of sedimentary basins. Subsidence patterns in coastal California basins imply complex evolution related to changing regional tectonics.

Compilation of published stratigraphic data allows construction of preliminary geohistory diagrams showing inferred rates of sediment accumulation within onshore California basins. Assumption of approximate porosity-depth functions for compaction of different lithologic types further permits calculation of adjusted- or decompacted-accumulation curves. Paleobathymetric estimates then define net-subsidence curves. Backstripping to compensate for local isostatic effects of sediment loading yields residual-subsidence curves, which are some measure of tectonic subsidence through time. The relative contributions of crustal thinning, thermal decay, and lithospheric flexure to overall tectonic subsidence are essentially unknown at present.

The following special problems are encountered in constructing geohistory diagrams for onshore California basins: (1) the uncertain duration and probable diachroneity of provincial foraminiferal "stages"; (2) the imprecision of paleobathymetric estimates based on foraminiferal paleoecology; (3) the paucity of available data on porosity-depth relations for siliceous sediments: and (4) the difficulty of compiling reliable composite columns by combining surface and subsurface sections.

Interpretations of geohistory curves offer the following general insights: (1) Sedimentation rates tended to remain constant regardless of changing bathymetry as long as overall tectonic settings of basins remained unchanged; therefore, rates of delivery of clastic sediment to local basins largely reflect rates of sediment production in nearby provenances. (2) The slopes of cumulative-subsidence curves are critically controlled by estimates of paleobathymetry; hence, patterns of subsidence during times when water was deep cannot be inferred reliably without accurate paleoecological control. (3) In comparison with other sources of error, different procedures for decompaction produce only minor variations in accumulation or subsidence curves, and the same is probably true for many other thick clastic successions.

Comparisons of geohistory curves offer the following regional insights: (1) The Laramide interval of shallow slab descent in latest Mesozoic and earliest Cenozoic time was apparently associated with regional uplift of the forearc region; uplift was followed by local subsidence within Paleogene basins, initiated by dextral shear along the proto-San Andreas system. (2) Mid-Tertiary subduction of young oceanic lithosphere on the east flank of the Pacific-Farallon ridge was apparently associated with a second phase of regional uplift of the forearc region; subsequent development of the San Andreas transform system was accompanied by local subsidence within Neogene basins. (3) Latest Miocene and younger pulses of local subsidence and uplift were probably related to wrench deformation and associated flexural effects adjacent to the current master trace or prominent splays of the San Andreas fault or associated thrusts.

Geohistory analysis (Van Hinte, 1978) is a powerful method for the study of subsidence patterns in sedimentary basins. A geohistory diagram shows the time-depth trajectories of selected stratigraphic horizons during accumulation of a given stratigraphic column. The preparation of geohistory diagrams requires knowledge of the age, thickness, and lithology of successive intervals of strata into which the column can be subdivided, as well as information about variations in paleobathymetry or paleotopography during deposition. The lithologic data are needed as a basis for decompaction, the process by which restored thicknesses for each stratigraphic interval are calculated for times in the past when overburden was less. Backstripping a stratigraphic column involves not only decompaction of constituent strata, but also isostatic unloading of the substratum (Steckler and Watts, 1978). If the isostatic depression of the substratum in response solely to the sediment load can be removed from the net subsidence, the magnitude and nature of tectonic effects on basin evolution can be gauged.

In this paper, we present approximate and partial geohistory analyses for selected sedimentary basins of onshore California (Fig. 1-1). We have deliberately restricted our analysis to data that are in the public domain and thus available to all. Our aim has been to develop the logical implications of accepted knowledge as a guide to improved concepts, rather than to produce definitive analyses. Our geohistory diagrams should be regarded, therefore, as preliminary graphs subject to revision by other workers who either acquire better data or interpret existing data in better ways. We conclude, nonetheless, that important overall relationships are revealed clearly by our treatment of the data.

SPECIAL PROBLEMS

The ideal subject for geohistory analysis is a continuously cored and logged well, for which detailed micropaleontologic and lithologic information is generated in a systematic and consistent manner. When the method is applied to outcrop sections and fragmentary well records that have been described for different purposes by multiple workers, comparative imprecision is bound to affect results. We accept this inherent handicap as the price that must be paid to bring the power of the method to bear on the interpretation of complex California sequences, whose full character has emerged only after years of study by teams of geoscientists. We also call attention, however, to the following special problems that arise in constructing geohistory diagrams for onshore California basins:

1. Fundamental age relations within Cenozoic squences of California are customarily reported mainly in terms of provincial foraminiferal stages, whose age ranges are not defined by standard global time scales. Moreover, certain of the provincial "stages" and "ages" are now widely regarded as diachronous to some degree. Figure 1-2 illustrates the somewhat arbitrary time-scale conventions that

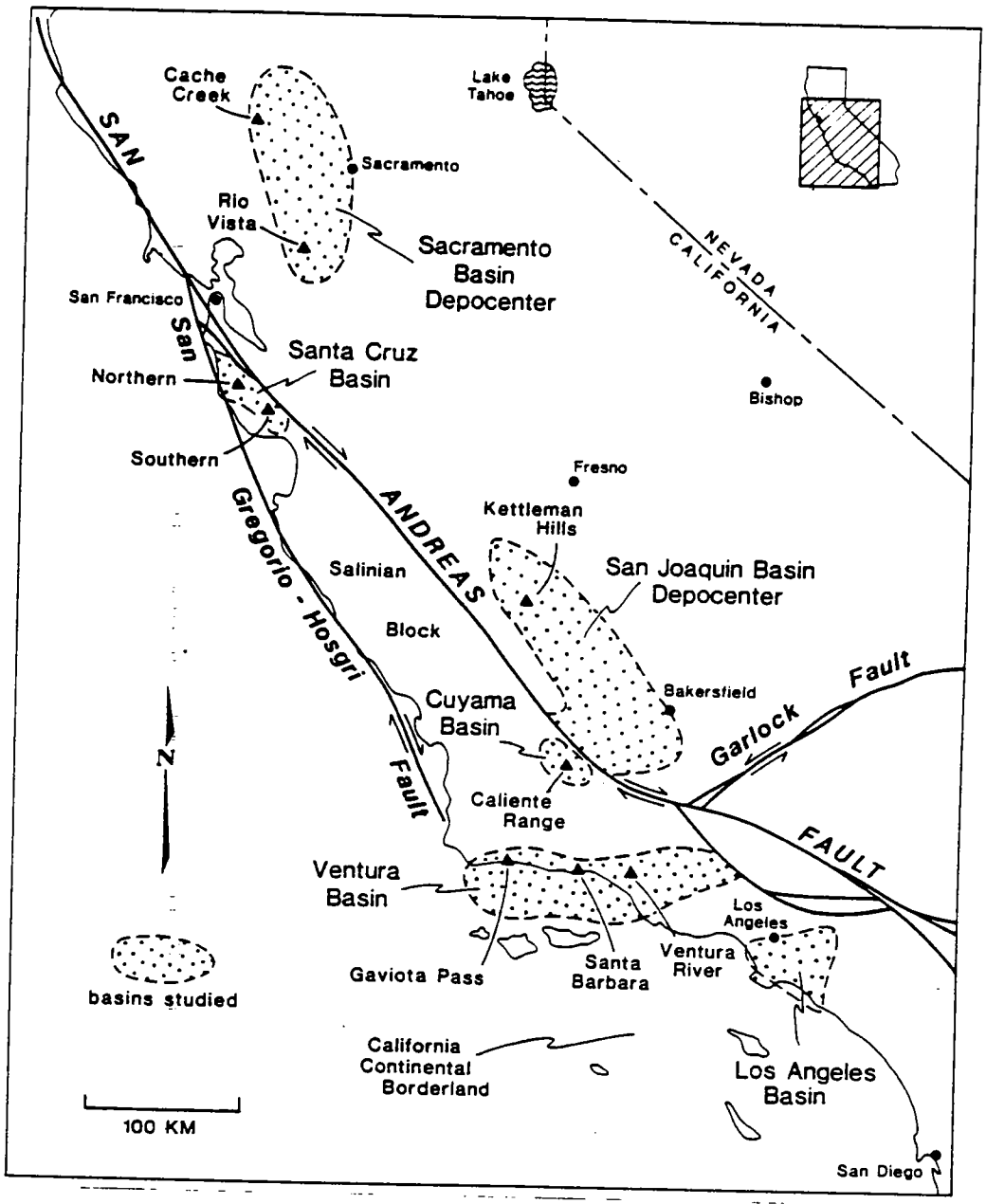

Fig. 1-1. Locations of California basins (stippled), for which geohistory analyses were made using stratigraphic columns from the sites indicated (triangles).

we adopted for the Cenozoic in this study. For Cretaceous stages and ages, we used the DNAG scale of GSA (Palmer, 1983). Future work will doubtless result in further improvement of both the Cretaceous and Tertiary time scales. However, our geohistory diagrams display no obviously anomalous features that might be interpreted as artifacts reflecting significant errors in the adopted time scale.

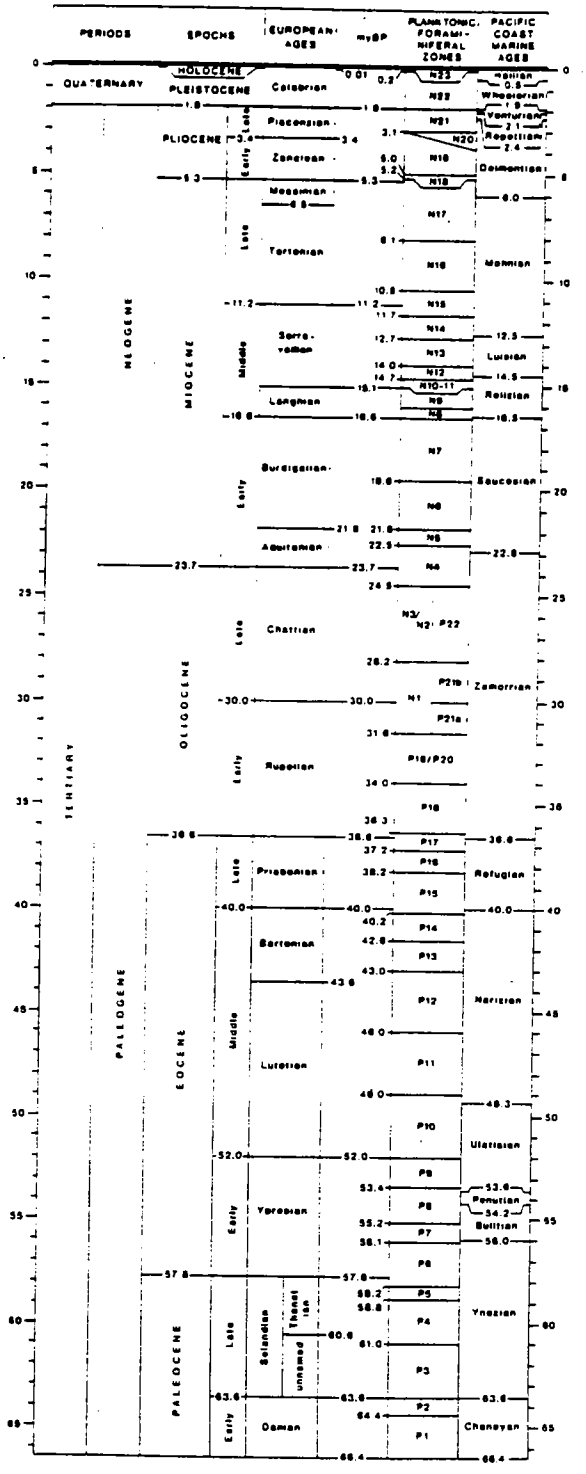

Fig. 1-2. Cenozoic time scale, including provincial California stage boundaries, adapted from Palmer (1983). Neogene from Berggren and Van Couvering (1974) with limits of Relizian and Luisian modified after Turner (1970). Paleogene after Berggren *et al.* (1985b) and Warren (1983).

2. Different workers define the boundaries between standard depth zones for benthic marine life forms at different levels below the sea surface (Bandy and Arnal, 1969; Van Hinte, 1978; Ingle, 1980; Kennett, 1982). As objective estimates of paleobathymetry are almost wholly dependent upon paleoecological interpretations, we needed a consistent scheme to use for translating faunal information into quantitative depth estimates. Accordingly, we adopted the following compromise depth ranges for the depth zones reported by micropaleontologists:

inner neritic	0–50 m
middle neritic	50–100 m
outer neritic	100–175 m
upper bathyal	175–600 m
middle bathyal	600–1500 m
lower bathyal	1500–3000 m
abyssal	3000–6000 m

We have little confidence in the strict validity of these depth values, but they serve to make our conclusions internally consistent. We suspect that the paleobathymetric aspects of our analysis are the weakest links in our chain of logic. As we lack personal expertise in micropaleontology, we followed published evaluations of paleobathymetry, but these are commonly either very general or partly contradictory.

3. Comprehensive porosity-depth curves for siliceous shales and porcelanites derived from impure diatomites were unavailable to us. As such strata form thick segments of several Tertiary formations in California, we developed an inferred porosity-depth curve (see below) based on knowledge of temperatures of inversion between pertinent silica phases and of typical geothermal gradients observed in the basins studied. Although we are confident that the relationship we used is more appropriate than a standard compaction curve for shale, we have no doubt that a more accurate expression could be derived from more data for these siliceous strata.

4. For many onshore California basins, a full appraisal of the sediment fill can be obtained only by joining two or more outcrop and/or well sections into a composite stratigraphic column. As many have noted in the past, this procedure is fraught with potential error. An older section concealed at depth beneath exposures of the younger part of a basin fill may not have the same thickness or lithology as correlative older strata exposed to view in another part of the basin. Any migration of depocenters through time serves also to ensure that most composite sections are unrealistic. We have been aware of this pitfall from the outset, and tried to make our composite sections as reliable as possible, but may still have produced misleading results in some cases.

GEOHISTORY CALCULATIONS

Age and thickness of strata are the most fundamental data for geohistory analysis. If nothing else is known, a cumulative-thickness curve can still be drawn showing "raw" rates of sediment accumulation unadjusted for the effects of compaction.

Next in importance are data on paleobathymetry (or paleotopography) and lithology. If changing paleodepth (or paleorelief) through time is known, rates and amounts of sediment accumulation can be converted to rates and amounts of subsidence (of the substratum). Lithologic information governs procedures for decompaction and backstripping because rates of compaction and porosity loss during burial vary with lithology.

In general, porosity reduction may occur by some combination of cementation (pore-space filling) and compaction, including pressolution. Both these diagenetic processes increase bulk density, but compaction also reduces volume, whereas cementation does not (Bond and Kominz, 1984). For simplicity, we assume that porosity reduction within a basin occurs exclusively by compaction, which reduces stratal thickness in strict proportion to the progressive reduction in porosity (Sclater and Christie, 1980; Watts, 1981). Although this assumption is surely invalid in detail, it represents a realistic approximation for any basin as a whole, for it is unlikely that cementing materials are derived in any significant proportion from outside the basin fill. It is probably most common for cementing materials to move from regions of excess pressolution at depth to shallower regions of net precipitation. If so, porosity-depth curves may tend to understate net compaction at deeper horizons and to overstate net compaction at shallower horizons.

From examination of empirical porosity-depth curves for various pertinent lithologies, we derived the following tentative porosity-depth formulas for lithologies present in California basins (in each case, the expression yields porosity in percent as a function of depth, Z, in meters: note that the expressions do not necessarily yield the best values for porosity at zero depth, but represent best-fit estimates for the full range of depths encountered):

siliceous shale:	$70/(1 + 0.002Z)$
shale/mudstone:	$60/(1 + 0.001Z)$
sandstone(undiff):	$50/(1 + 0.0005Z)$
quartz sandstone:	$90/(2 + 0.00075Z)$
arkosic sandstone:	$\exp(4.0 - 0.00038Z)$
lithic sandstone:	$\exp(3.7 - 0.00030Z)$

Using these or analogous expressions, decompacted thicknesses for each stratigraphic interval within a given stratigraphic column can be calculated for different times in the past by successively backstripping overlying stratigraphic units. In essence, the procedure involves "sliding" each stratigraphic interval "up" the appropriate porosity-depth curve in depth increments coordinate with the successive time steps. In practice, this was done using a computer program, whereby each stratigraphic interval could be apportioned among the six lithologies represented. Figure 1-3 shows the symbols used to designate different lithologic types on geohistory diagrams. As a rough approximation, massive volcanics were decompacted as if they were quartz sandstones, which are also relatively resistant to compaction.

When an isostatic correction is applied during backstripping to remove the effects of progressive sediment loading on the elevation of the substratum, the

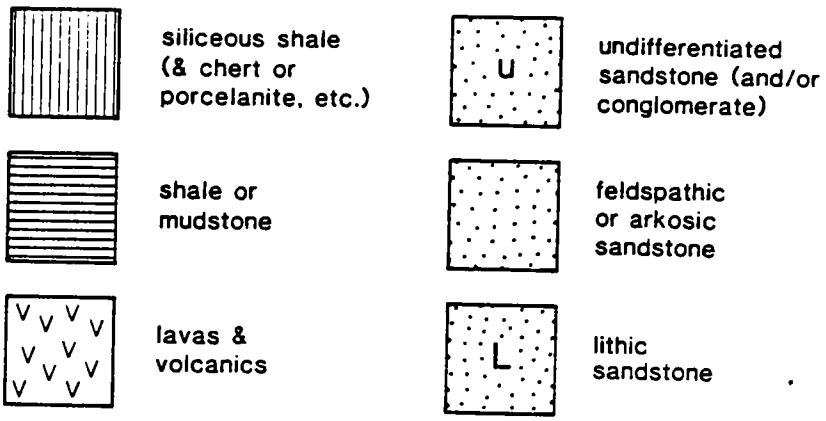

Fig. 1-3. Symbols used to depict key lithologic types on geohistory diagrams (see text for discussion).

resulting subsidence curve is commonly termed the "tectonic" subsidence curve (Steckler and Watts, 1978; Bond and Kominz, 1984). In general, such isostatic restorations should take into account the flexural response of the lithosphere. At this stage of investigation in most California basins, however, it is not possible to select flexural parameters intelligently. We have instead determined isostatic response as if all sediment loads were compensated locally (i.e., simple Airy model). We refer to subsidence curves from which this nominal Airy isostatic value has been removed as "residual" subsidence curves. This residual subsidence may incorporate effects of crustal thinning, thermal decay, and flexural behavior in varying proportions.

At each step in the backstripping process, the Airy isostatic effect of each stratigraphic interval in a stratigraphic column is calculated by our program in terms of decompacted sediment thickness and calculated mean sediment density. Mean sediment density is determined from assumed grain density (2.65) and hindcast porosity (water-filled). Isostatic balance is taken relative to mantle density (3.33). The program yields values for water-loaded (i.e., not air-loaded) residual subsidence.

GEOHISTORY PLOTS

Geohistory diagrams are conventionally plotted (as in Fig. 1-4) with the depth ordinate increasing downward, and with the age abscissa decreasing toward the right, where the present stratigraphic column is plotted to indicate the nature of the basic data set. For ease of interpretation, paleodepth (of water) or paleorelief is customarily plotted across the top of the diagram to indicate in a graphic way the changing elevation of the top of the evolving sediment column through time. By this convention, curves of both "raw" (unadjusted) and decompacted cumulative subsidence incorporate paleobathymetric interpretations "above" representations of sediment thickness. Thus, paleodepth occupies its "correct" space on top of the growing sediment column.

Where paleobathymetric interpretations are imprecise or questionable, we have found it convenient to pursue a different plotting procedure (as in Fig. 1-5), whereby paleodepth is not shown at the top of the diagram. Instead, we first plot cumulative sediment thickness, both "raw" (unadjusted) and decompacted, by hanging the top of the growing sediment column to the top of the geohistory diagram. In this way, we define rates of sediment accumulation through time, independent of paleobathymetry or subsidence rate. To obtain subsidence curves, we then add estimates for means or ranges of paleobathymetry to the bottoms of the sediment-accumulation curves. The resulting plots are more awkward to read than the standard format in cases where paleobathymetric variations are minor. However, they honor the comparative quality of the data in cases where uncertainties in paleobathymetric interpretations dominate inferences about subsidence or uplift of deep basin floors.

Curves of residual subsidence can be constructed for mean estimates or for estimated ranges of paleobathymetry. Where paleobathymetric uncertainties are large, the constraints on residual-subsidence curves may be quite loose. Where sedimentary sequences of unknown thickness and uncertain lithology underlie the oldest horizon depicted on a geohistory diagram, the residual-subsidence curve may also include a component representing continued compaction of the subjacent sediment.

Components of residual subsidence curves derived from errors in paleobathymetry or decompaction are nontectonic, but otherwise, the residual-subsidence curves provide a rough indication of tectonic influences on basin evolution. In the California setting, tectonic controls on subsidence might logically include: (1) changes in thermal conditions and density relations within the forearc mantle profile; (2) crustal thinning and thermal decay beneath transtensional pull-apart basins; and (3) lithospheric flexure beneath tectonic loads associated with transpressional structures. At present, no effective means exist to distinguish clearly among these possible influences on basin evolution.

Because isostatic compensation of sediment loads actually involves flexure of the lithosphere, residual-subsidence curves based on the concept of strictly local isostatic compensation cannot accurately measure other tectonic influences. In the thickest depocenters, residual-subsidence curves based on local Airy compensation tend to understate the amount of fundamental tectonic subsidence. This is generally true because the isostatic effects of the local sediment load are actually spread over a wide area of flexure, rather than being restricted to the immediate substratum, as assumed in the Airy model. Conversely, the residual Airy curves tend to overstate the amount of tectonic subsidence at basin flanks, where no subsidence at all might occur were it not for the flexing sediment load within the keel of the basin.

Cuyama Basin

Figure 1-4 is a geohistory diagram for the petroliferous Cuyama basin (Fig. 1-1), a small "pocket" basin near the juncture between the Coast Ranges and the Transverse Ranges (also, see Lagoe, this volume). Thicknesses and lithologies are

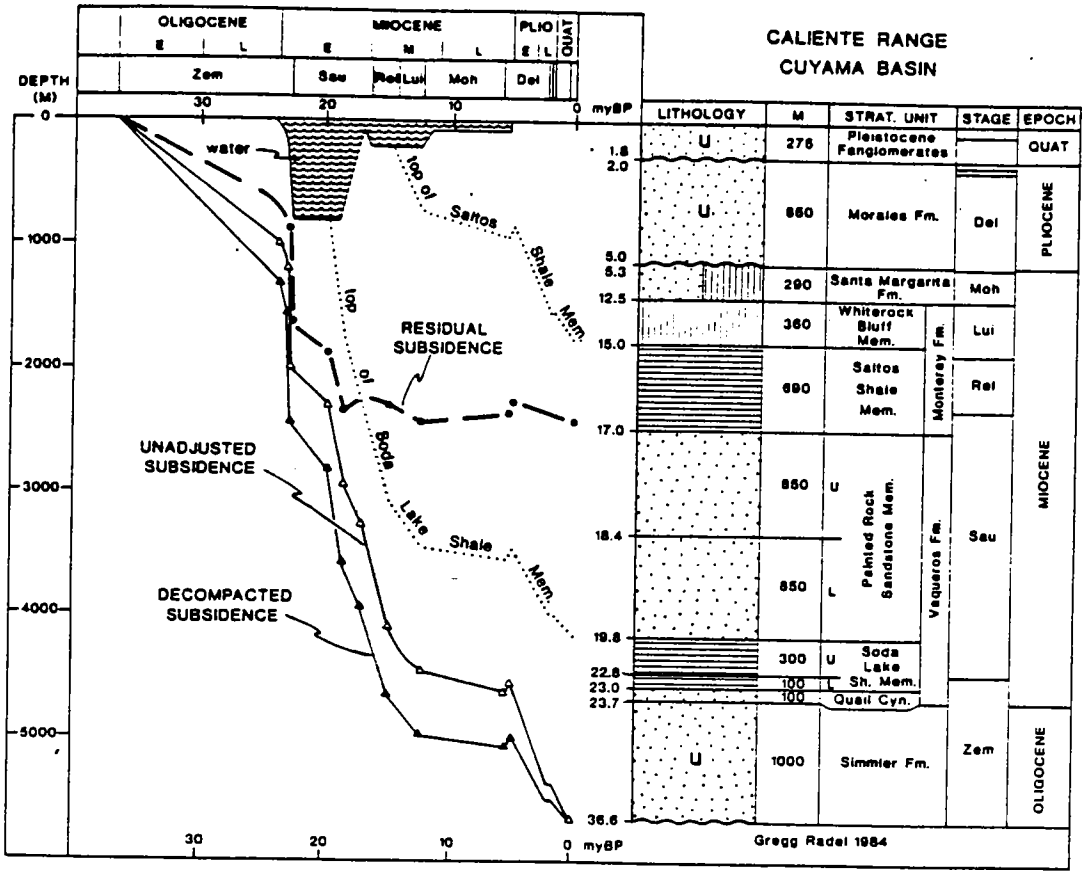

Fig. 1-4. Geohistory diagram for Caliente Range in Cuyama basin. Curves plotted in conventional format (see text). Most stratigraphic data from Hill *et al.* (1958), Woodburne (1975), and Bartow (1978). Supplemental subsidence curves shown for the tops of the Saltos and Soda Lake shale units are decompacted curves.

based on the essentially intact outcrop section of the Caliente Range. Note how the decompacted-subsidence curve for the base of the Oligocene section diverges downward from the unadjusted-subsidence curve, only to rejoin the latter at the vertical line representing the present time. This is the expected behavior of two such curves in all cases, for decompacted sediment thicknesses are uniformly greater than present sediment thicknesses.

The residual-subsidence curve implies rapid tectonic deepening of the Cuyama basin at the beginning of the Early Miocene (25–20 my B.P.). Especially rapid sedimentation at peak rates near 500 m/my occurred slightly later (20–15 my B.P.), in the Early to Middle Miocene. The marked tectonic deepening is inferred, even though we depict quite conservative water depths in the upper-bathyal zone for lower parts of the Vaqueros Formation. The subsequent history of the basin seemingly has involved mainly sedimentary infilling of the deep hole thus formed, and compensatory isostatic subsidence of the substratum under the

growing sediment load. This mode of Neogene evolution is reflected by the divergence of the curves for sediment accumulation from the residual-subsidence curve, which is subhorizontal. If the Early Miocene basin was actually deeper than we have shown, as some workers would argue, then the subsequent history of the basin apparently must have involved intra-Miocene tectonic uplift of the basin floor to achieve the shallow water depths recorded by Upper Miocene strata. However, our inferences about Miocene water depths are generally compatible with the recent interpretations of Lagoe (1984), although our plot was not coordinated in detail with his results.

The dramatic episode of subsidence near the boundary between the Oligocene and the Miocene may have been triggered by crustal thinning during pull-apart rifting. Andrews and Pitman (1984) argue that rapid lateral heat loss from the substratum of small transtensional basins may allow unusually abrupt sinking that is not delayed by the need for slow thermal decay. The timing of such inferred extensional deformation may have been controlled by the passage of an unstable triple junction along the California continental margin. Such a triple junction was located at the northern end of the nascent San Andreas transform, and passed the latitude of the Cuyama basin near the end of the Oligocene, about 25 my B.P. (Fig. 8 of Dickinson and Synder, 1979).

Sacramento Basin

Figure 1-5 is a geohistory diagram for the Cretaceous part of the Great Valley Group (Ingersoll and Dickinson, 1981) in the western part of the Sacramento Valley. As the stratigraphic column is a composite of outcrop and well sections located about 100 km apart along regional strike (see Fig. 1-1), the total thickness may be exaggerated somewhat. The sequence is overlain in the subsurface by about 1500 m of Cenozoic strata. Consequently, curves for unadjusted and decompacted cumulative sediment accumulation do not merge at their younger ends, shown here near the boundary between the Cretaceous and the Tertiary.

Deposition of the thick clastic sequence occurred in a deep forearc trough of the late Mesozoic arc-trench gap along the California continental margin (Ingersoll, 1978a). Gradual filling of the forearc basin is inferred through most of the Cretaceous, followed by rapid shoaling during the Maastrichtian. Continuous deposition ended by mid-Paleocene time, and several unconformities are present within the overlying Tertiary section.

The geohistory plot (Fig. 1-5) places prime emphasis on rates of sediment accumulation, which apparently increased in mid-Cretaceous time from about 100 m/my in the Early Cretaceous to about 250 m/my in the Late Cretaceous (Ingersoll, 1979). The more slowly deposited Lower Cretaceous units are mainly slope and basin-plain deposits, whereas the more rapidly deposited Upper Cretaceous units are largely submarine-fan deposits (Ingersoll, 1978a, 1982a).

Paleobathymetric interpretations present an unresolved challenge for all units below the Sacramento Shale. The underlying strata are all turbidites that probably formed below the carbonate compensation depth (Ingersoll, 1976, 1979). The Cretaceous CCD has been estimated at about 4000 m for the open oceans (Van

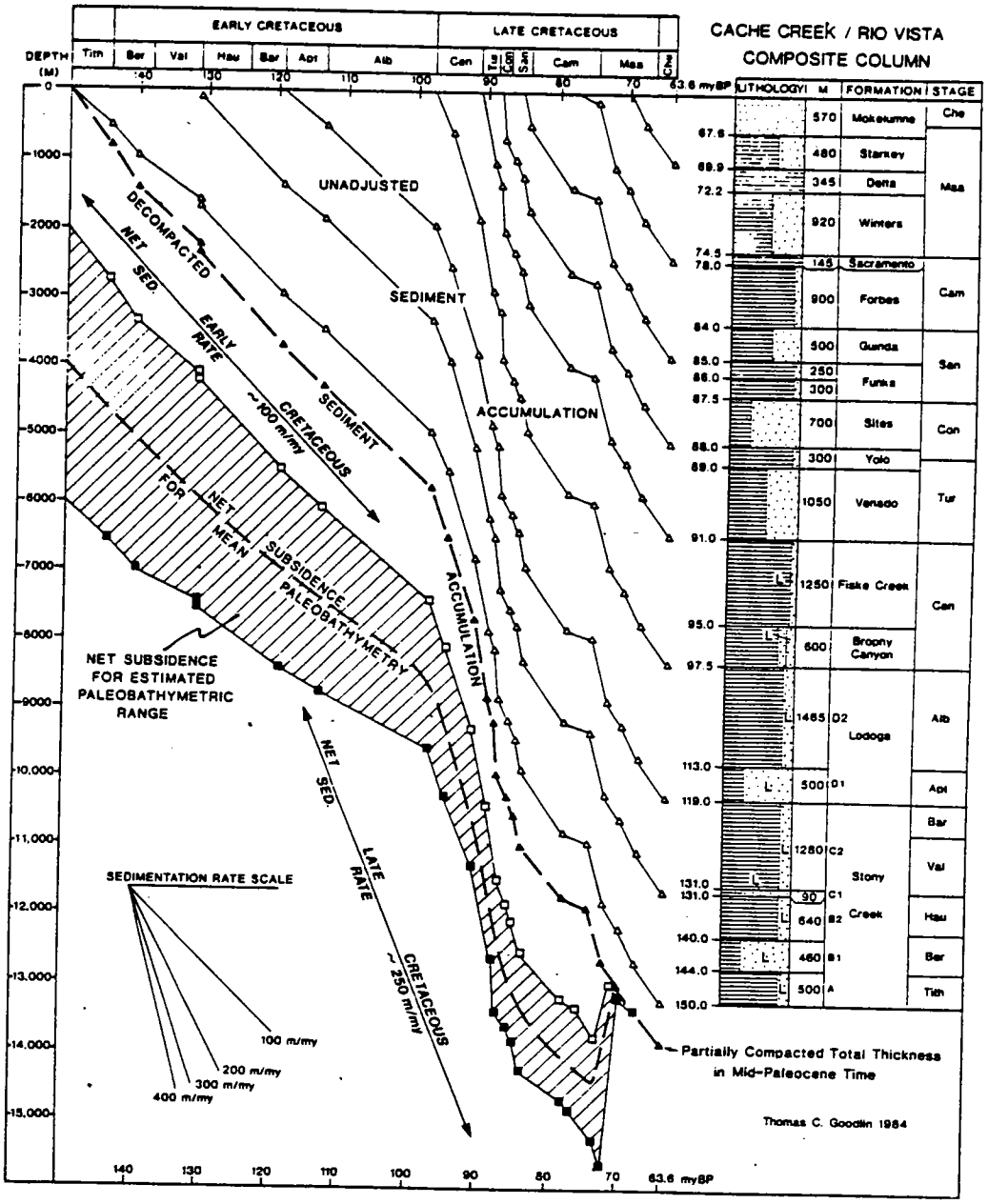

Fig. 1-5. Geohistory diagram for Cretaceous strata of Sacramento basin. Curves plotted in unconventional format (see text). Composite stratigraphic column taken from outcrop section along Cache Creek (75 km WNW of Sacramento) for Forbes Formation downward (Ojakangas, 1964, 1968; Ingersoll, 1976, 1979), and from well section (SOCAL Peter Cook 15, sec 8, T4N, R3E) near Rio Vista (40 km SSW of Sacramento) for Forbes Formation upward (Cherven, 1981, 1983c).

Andel, 1975), but its nearshore depth may well have been different. We have arbitrarily taken the depth of the sediment-water interface as 2000–6000 m (mean estimate of 4000 m) in the latest Jurassic, and have assumed that it shoaled steadily at a constant rate to achieve the lower-bathyal depth recorded for the Sacramento Shale (Cherven, 1983c). These assumptions imply net cumulative subsidence of roughly 10 km (7.5–12.5 km) within the forearc basin during the Cretaceous. This value might be reduced somewhat if we have erroneously summed the thicknesses of overlapping depocenters in constructing the stratigraphic column for the basin.

Because of the gross uncertainties in paleobathymetry, we have not plotted a residual-subsidence curve. For the assumed range in paleobathymetry, however, the residual-subsidence curve might be subhorizontal from the Tithonian to the Campanian (see Fig. 1-5). This result would imply that subsidence during most of the deposition of the Great Valley Group was entirely isostatic in response to the sedimentary infilling of an initially deep forearc basin. Thus, no tectonic subsidence of the Cretaceous forearc is required, given the initial existence of a deep trough floored by oceanic crust within the arc-trench gap.

Above the Sacramento Shale, the progradational fan-slope-delta succession of the Winters-Delta-Starkey sequence documents rapid shoaling of the Sacramento basin, leading to deposition of the fluvial Mokelumne Formation (Cherven, 1983c). The transition from lower-bathyal depths to sea level took place within about 7.5 my, while a thickness of less than 1750 m of strata accumulated. Unless we have significantly overestimated the depth of lower-bathyal environments, this shoaling of the basin required abrupt tectonic uplift of the basin floor during Maastrichtian time (a conclusion first suggested to us by S. A. Graham).

The apparent initiation of uplift at about 75 my B.P. coincides roughly with the onset of the Laramide orogeny inland (Coney, 1972). If the Laramide orogeny was triggered by shallow slab descent beneath the continental margin (Dickinson and Snyder, 1978), uplift within the forearc basin may have been caused by the insertion of buoyant subducted lithosphere into the mantle beneath the forearc region. The presence of such a buoyant slab beneath the forearc region would have lowered net mantle density, and thus, changed the conditions for overall isostatic balance of the forearc sediment load.

Ventura Basin

Elongate east-west, the Ventura basin lies between the Santa Ynez Mountains on the north, and the Santa Monica Mountains and Channel Islands to the south (also, see Ogle *et al.*, this volume). As part of the western Transverse Ranges, the Ventura basin has been involved in major crustal rotations of dextral sense during the Neogene (Luyendyk *et al.*, 1980; Luyendyk and Hornafius, this volume). For comparative purposes, we have prepared geohistory diagrams for three segments of the basin along strike near the coast in the Ventura River, Santa Barbara, and Gaviota Pass areas (Fig. 1-1). We have treated only the Cenozoic strata of the basin, although unknown thicknesses of Cretaceous strata underlie them.

Although outcrop sections are essentially continuous with subsurface sections, both onshore and offshore, the likelihood of migratory depocenters during

Tertiary sedimentation suggests that our stratigraphic columns are actually composite sections. Total thicknesses, thus, may not be representative of any single site within the basin. However, pulses of sedimentation and or subsidence indicated by geohistory analysis all must pertain to some part of the composite basin, even though it may be that no part of the basin experienced all of them.

Figure 1-6 for the Ventura River area indicates a nearly constant overall rate of sediment accumulation at about 150 m/my during most of Tertiary time. The sedimentation rate then increased markedly in the Pliocene until arrested by Quaternary uplift. The Pliocene pulse of sedimentation seemingly coincided roughly with the shift of the path of the San Andreas transform from the edge of the continental block into the Gulf of California, and thence northward along the present course of the San Andreas fault. Conceivably, successive flexural downwarping and upwarping of the basin floor (to produce Pliocene subsidence followed by Quaternary uplift) may have occurred as the western Transverse Ranges were deformed along the margin of the Pacific plate.

Inferences about earlier subsidence are largely dependent upon inferences about paleobathymetry. We have accepted the conservative estimates of Link and Welton (1982) for Paleogene paleobathymetry. Consquently, the curve for net subsidence in the Ventura River area has a nearly constant slope from Paleocene to Miocene time. However, the residual-subsidence curve includes a flattened mid-Tertiary segment that appears to separate discrete pulses of Paleogene and Neogene subsidence having presumably different tectonic origins. Had we adopted the deeper paleobathymetric estimates of Ingle (1980) for Paleogene strata, the curve for residual subsidence would display more marked upward concavity for the Paleogene, and consequently, more marked mid-Tertiary flattening. In any case, reduced mid-Tertiary rates of tectonic subsidence were evidently preceded and followed by Paleogene and Miocene episodes of comparatively rapid tectonic subsidence.

Farther west, near Santa Barbara (Fig. 1-7) and Gaviota Pass (Fig. 1-8), subsidence relations within the Ventura basin were similar, but different in detail. Total sediment accumulation was only about half that observed for the Ventura River area, and sediment accumulation rates were only about 100 m/my prior to enhanced rates of Pliocene sedimentation. This observation reflects the fact that these two western sites are along the northern flank of the basin, whose keel is offshore (Curran *et al.*, 1971). The pattern of mid-Tertiary subsidence is even more anomalous than for the Ventura River area. At Gaviota Pass (Fig. 1-8), our interpretation implies a virtual stillstand in residual or tectonic subsidence for about 25 my in the Eocene and Oligocene. The amount of apparent uplift of the substratum shown near the Eocene-Oligocene time boundary is probably within the range of magnitude that could reflect a eustatic drop in sea level (also, see May and Warme, this volume).

The fundamental causes for the seemingly discrete pulses of Paleogene and Miocene subsidence in the Ventura basin are still largely speculative. Their apparent timings permit the hypothesis that they were produced by transform tectonics related to the proto-San Andreas and San Andreas faults, respectively. Rapid tectonic subsidence in the interval 60–55 my B.P. immediately followed the

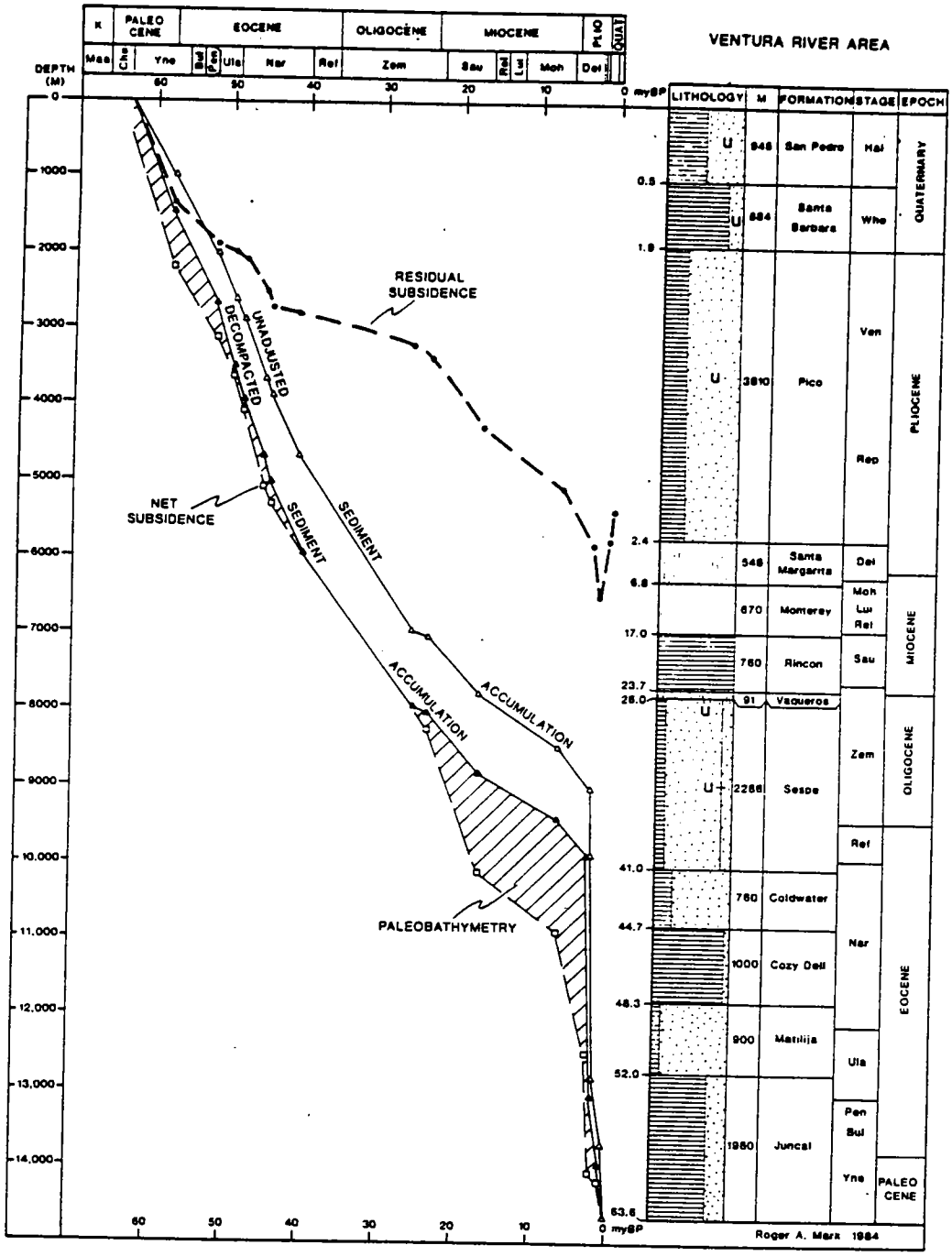

Fig. 1-6. Geohistory diagram for Ventura River area of Ventura basin. Stratigraphy after Bailey (1947), Dibblee (1966), Stauffer (1967b), Curran *et al.* (1971), Ingle (1980), and Link and Welton (1982). Paleobathymetry after Link and Welton (1982) for Paleogene, and Ingle (1980) for Neogene.

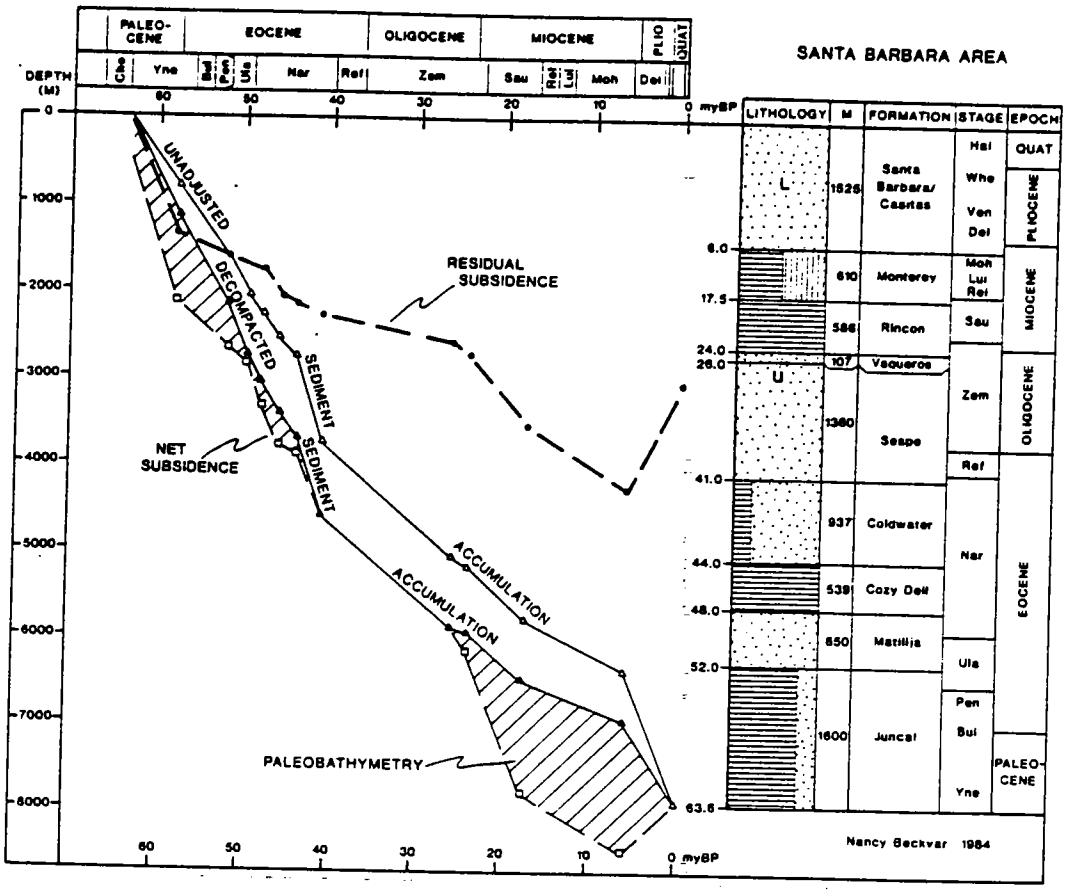

Fig. 1-7. Geohistory diagram for Santa Barbara area of Ventura basin. Stratigraphy after Dibblee (1966), Stauffer (1967a,b), Van de Kamp *et al.* (1974), and Ingle (1980). Paleobathymetry after Link and Welton (1982) for Paleogene, and Ingle (1980) for Neogene.

most likely time for motions along the proto-San Andreas fault (Dickinson *et al.*, 1979). Rapid tectonic subsidence beginning about 25 my B.P., or slightly before, coincided well with the passage of an unstable triple junction marking the northern end of the evolving San Andreas transform (Dickinson and Snyder, 1979).

From a comprehensive analysis of fault kinematics in southern California, Bird and Rosenstock (1984) have recently argued that a dense slab of partly subducted lithosphere has been underthrust from the south beneath the Transverse Ranges since the beginning of Pliocene time. The flexural effects of this subcrustal mass, coupled with the crustal load of associated thrust sheets, may have contributed to subsidence within the Ventura basin.

Santa Cruz Basin

The Santa Cruz basin (Figs. 1-9 and 1-10) is a linear trough adjacent to the San Andreas fault (Fig. 1-1). No pre-Tertiary sequences are known within the basin.

but Paleogene units were contiguous at the time of deposition with strata that rest partly on Cretaceous rocks in the Temblor Range (Clarke and Nilsen, 1973). Paleontologic control for both age and paleobathymetry within the Santa Cruz basin is probably as good as the literature offers for a Tertiary basin in California.

Unconformities divide the Tertiary sequence into four distinct packets of strata. Oldest is a thin Paleocene unit only locally exposed. The thickest package ranges from Early Eocene to Early Miocene in age. Middle Miocene and Upper Miocene to Pliocene successions complete the column. The presence of multiple unconformities attests to a complex tectonic history.

Rapid subsidence and sediment accumulation in Early to Middle Eocene time essentially initiated the Santa Cruz basin. This phase of deposition may record the development of a structurally and topographically complex continental borderland related to Paleocene deformation within the proto-San Andreas system (Nilsen and Clarke, 1975). If so, the early Santa Cruz basin can be regarded basically as a pull-apart structure produced by proto-San Andreas deformation.

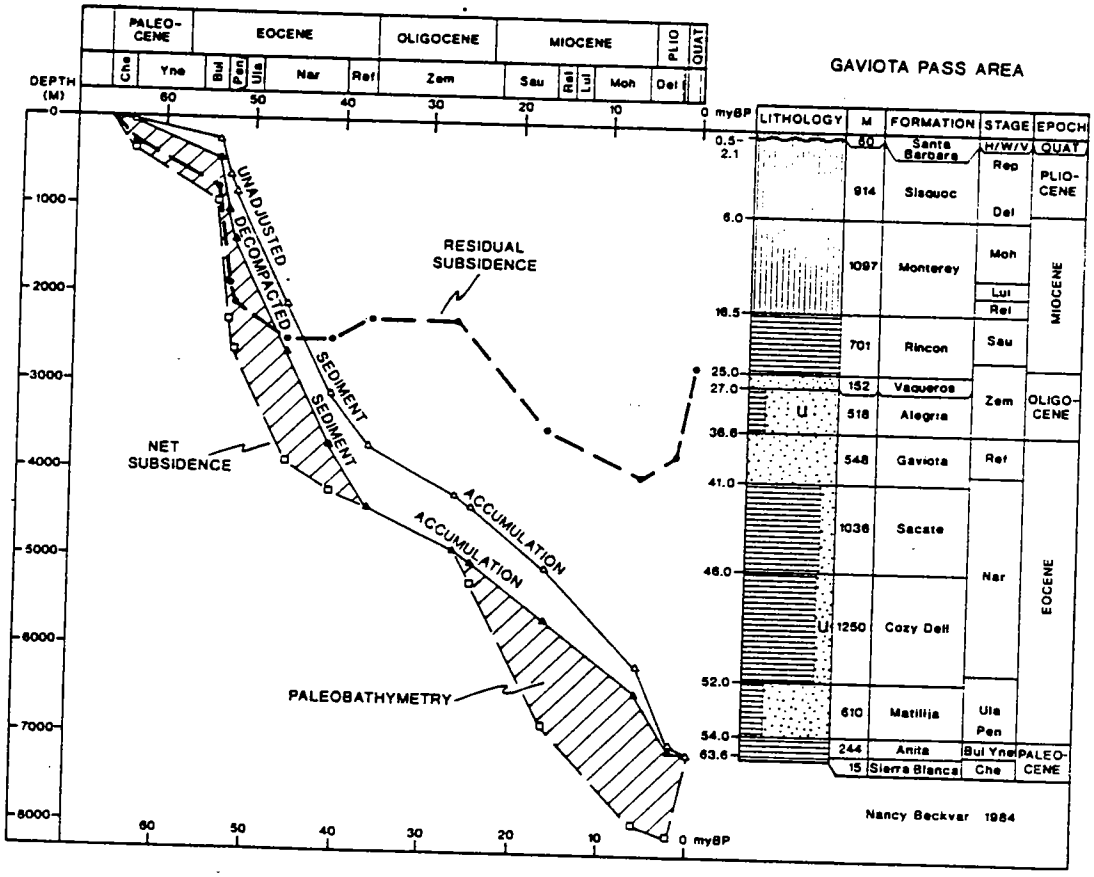

Fig. 1-8. Geohistory diagram for Gaviota Pass area of Ventura basin. Data modified after Ingle (1980) using Stauffer (1967a) and Van de Kamp *et al.* (1974).

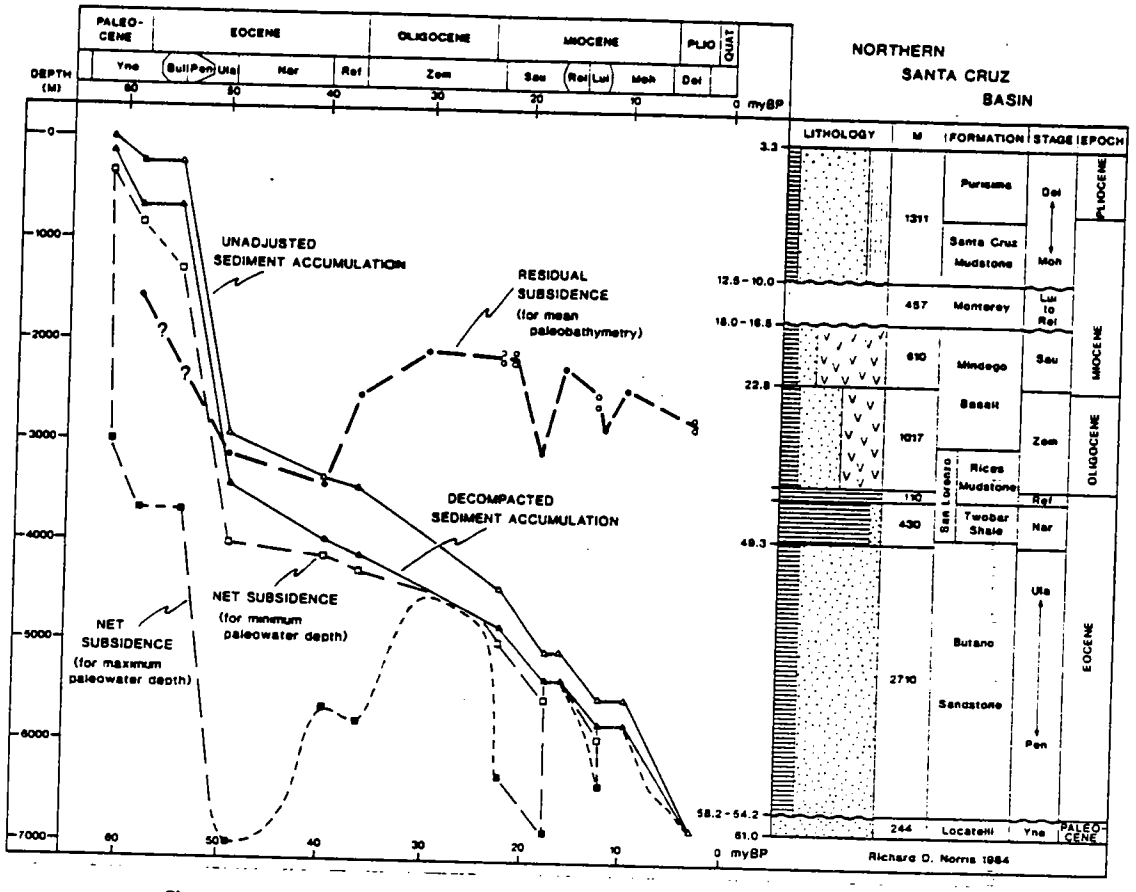

Fig. 1-9. Geohistory diagram for northern Santa Cruz basin. Data after Cummings *et al.* (1962).

As sedimentation continued at reduced rates from Middle Eocene to mid-Oligocene time, best estimates of paleobathymetry imply gradual uplift of the basin floor. This result is indicated by a reversal in the slope of the residual-subsidence curve, which is a rough measure of "tectonic" subsidence (Fig. 1-11). Although such uplift could have been due to local tectonics (Clark and Rietman, 1973), it may reflect regional trends in basin evolution. A slowdown or actual reversal in subsidence during the same time period was also detected for the Ventura basin.

Nilsen (1984a) has inferred that widespread uplift of the California forearc region occurred during the Late Eocene and Early Oligocene in response to subduction of progressively younger and more buoyant oceanic lithosphere. The age pattern of descending oceanic lithosphere must have changed in this fashion as the continental margin encroached upon the flank of the Pacific-Farallon rise crest prior to development of the San Andreas transform system (also, see Nilsen, this volume).

Nontectonic explanations for the behavior of the residual-subsidence curve in the mid-Tertiary are difficult to sustain. The amount of relative change in sea

level required to explain the shape of the curve seems excessive to ascribe to eustatic fluctuation. The limits of potential error in estimates of probable paleobathymetry are marginally capable of bringing the residual subsidence curve to a subhorizontal position (Fig. 1-11). If this proves to be the correct resolution of the issue, it would mean that current paleobathymetric estimates have a systematic bias toward interpretations of deeper water than was actually present in California basins.

Beginning in the Early Miocene, the Neogene Santa Cruz basin experienced several rapid episodes of subsidence and uplift. These events can be ascribed to pull-part behavior and wrench deformation associated with the San Andreas transform system. The most abrupt pulse of subsidence can be correlated roughly with the passage of the unstable triple junction at the northern end of the San Andreas transform along the adjacent continental margin about 20 my B.P. (Dickinson and Snyder, 1979). Voluminous basaltic eruptions in the Early Miocene suggest significant local extensional tectonics at the time that the triple junction was in the vicinity of the Santa Cruz basin. Middle Miocene uplift recorded by

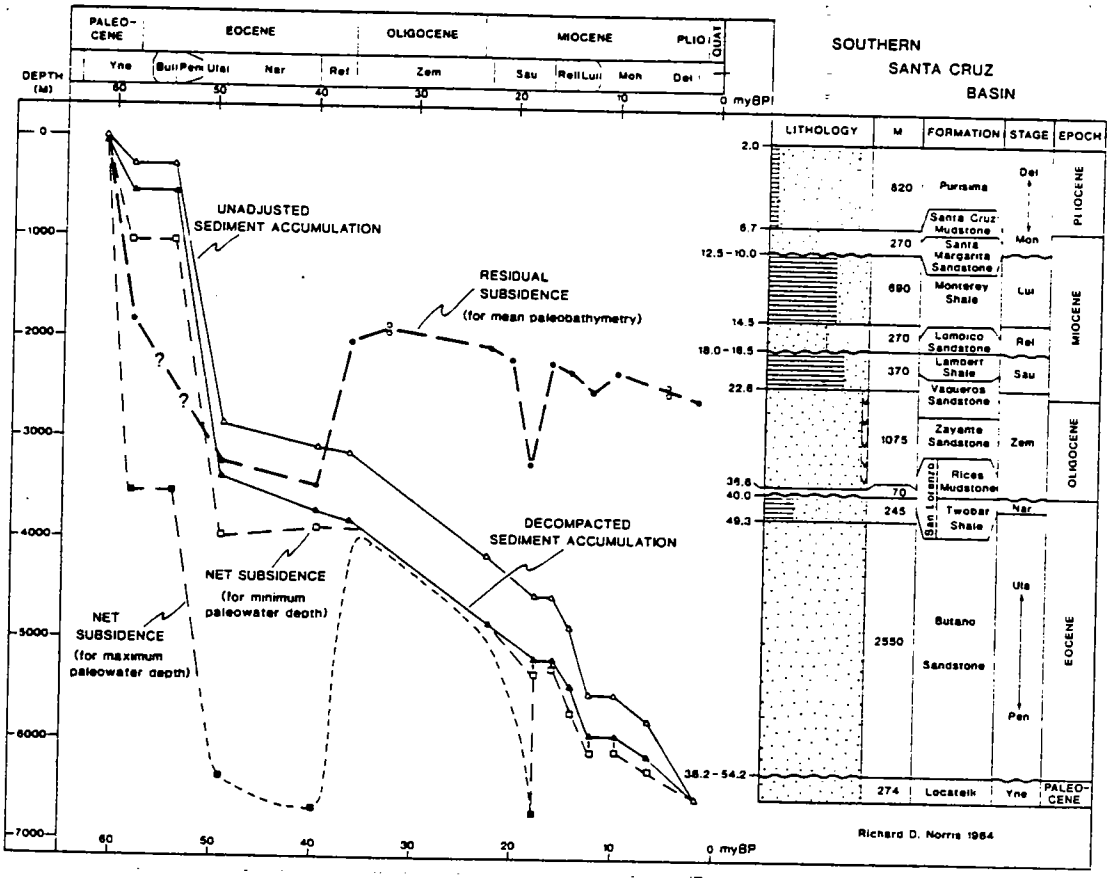

Fig. 1-10. Geohistory diagram for southern Santa Cruz basin. Data after Clark (1981).

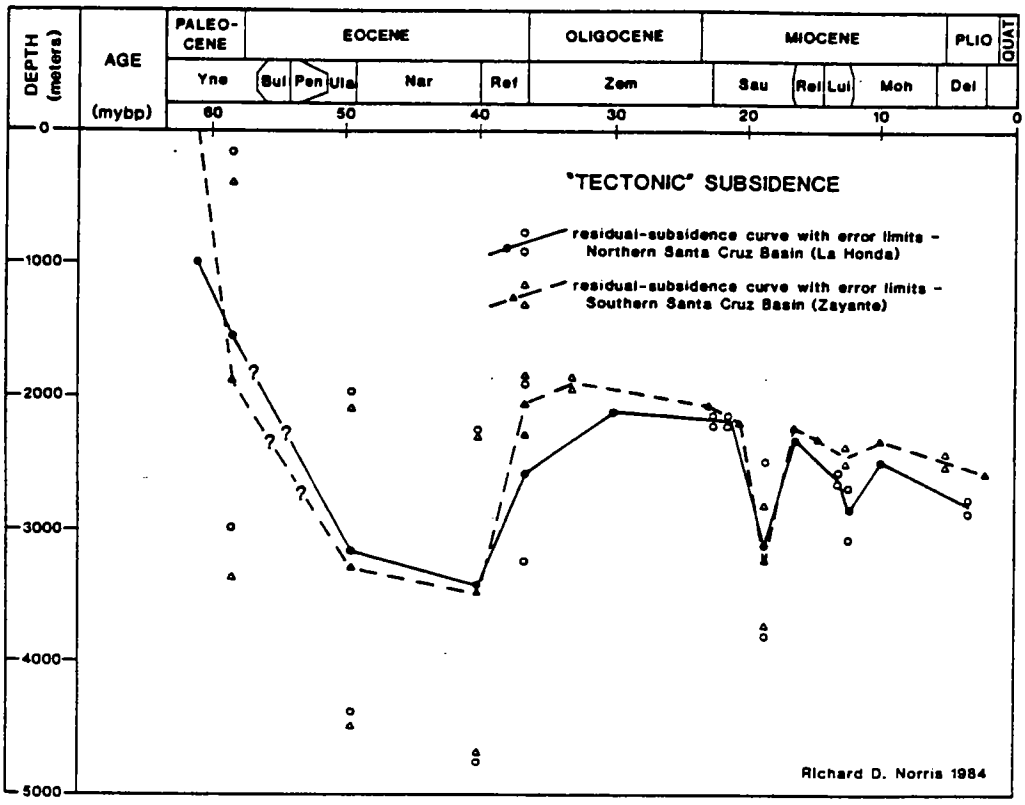

Fig. 1-11. Comparison of curves of residual "tectonic" subsidence for northern and southern parts of Santa Cruz basin (see Figs. 1-9 and 1-10).

unconformities in the Santa Cruz basin may reflect the coordinate onset of wrench deformation within the Salinian block (Graham, 1978).

Net residual subsidence since the Oligocene has been slight within the parts of the Santa Cruz basin represented by the geohistory diagrams (Figs. 1-9 and 1-10). However, nearly 5000 m of strata have been deposited in the last 10–12 my near the coast adjacent to the San Gregorio fault (Fig. 1-1). Their presence suggests that late Neogene subsidence in the coastal Santa Cruz basin may have been related to wrench deformation of the block between the San Andreas and San Gregorio faults.

San Joaquin Basin

A geohistory diagram (Fig. 1-12) for the area around Reef Ridge and the Kettleman Hills along the western side of the San Joaquin basin (Fig. 1-1) shows the severe dependence of inferred tectonic subsidence in California Tertiary basins on estimates of changing paleobathymetry through time. In this instance, paleoecology is the key to paleotectonics. The curves for unadjusted and for decompacted sediment accumulation betray no hint of the dramatic vertical

motions of the basin floor required by the inferred paleobathymetry (also, see Graham, this volume, and Bartow, this volume).

Curves of cumulative sediment accumulation indicate rapid sedimentation rates during the Cretaceous, but slower sedimentation rates during the Paleogene, and a hiatus at an Oligocene unconformity. Neogene rates of sediment accumulation gradually increased through the Miocene to culminate in the Pliocene and Pleistocene. By inference, without information on paleobathymetry, the upward concave Cretaceous-Paleogene curve might appear to reflect thermotectonic subsidence in a rifted basin, whereas the upward convex Neogene curve might be ascribed to progressive flexure within an orogenic basin.

Paleobathymetric interpretations imply that the true subsidence pattern was considerably more complicated. The plotted Cretaceous data are highly questionable (as discussed above), but the Cenozoic data are thought to be generally valid within the limits of uncertainty shown. Three periods, during which deep water is inferred, define distinct pulses of presumed subsidence and uplift. These paleoecologically determined pulses of vertical movement completely dominate the

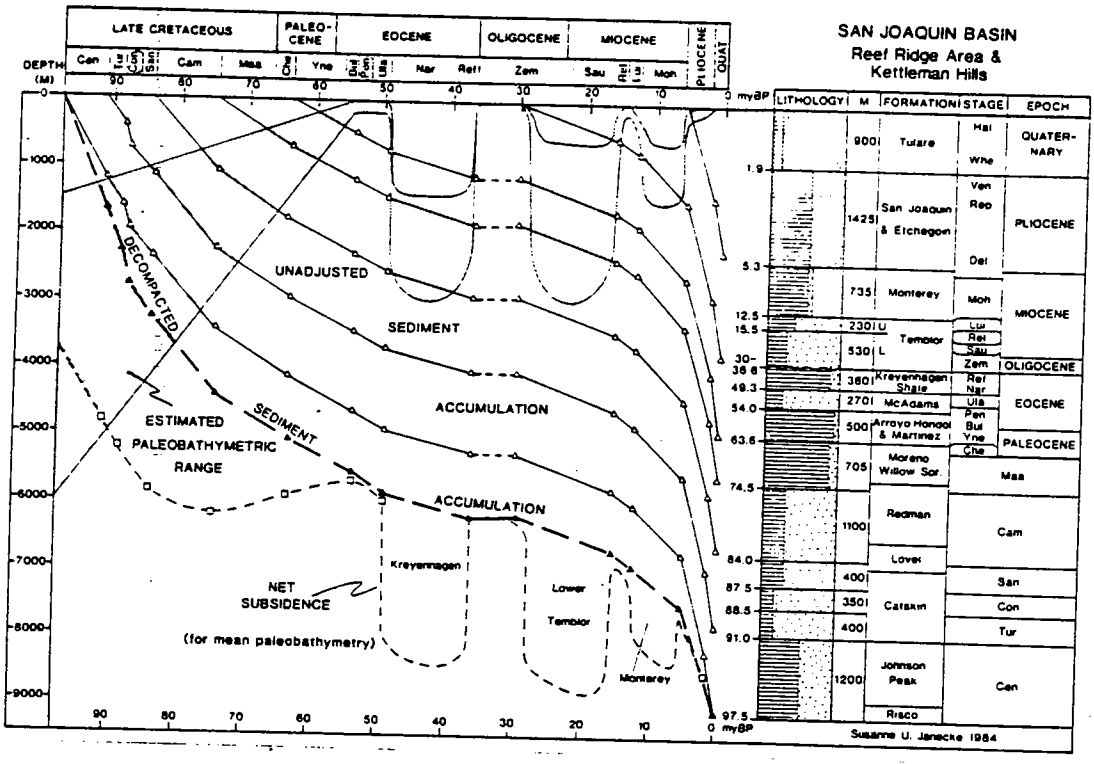

Fig. 1-12. Geohistory diagram for a composite stratigraphic column representing the outcropping Cretaceous section of Reef Ridge (Dibblee, 1973b; Ingersoll, 1976) and the subsurface Cenozoic section of the Kettleman Hills (Woodring *et al.*, 1940; Harding, 1976; and California Division of Oil and Gas Summary of Operations Reports). Paleobathymetry from Bandy and Arnal (1969), Addicott (1972a, 1973), Clarke (1973), and Stanton and Dodd (1976). Lithology partly from Marsh (1960) and Anderson (1972).

local curve for net cumulative subsidence during the Cenozoic. Moreover, we have tended to be conservative in the plotted water depths. Our purpose here is not to argue for the validity of the inferred paleobathymetry in detail, but simply to show that rather standard interpretations lead directly to dramatic tectonic implications that cannot be sensed in any other way.

Geohistory diagrams thus highlight in a graphic manner the significance of paleoecological studies for basin analysis in tectonically active regions. The situation underscores the need to develop careful procedures for determining paleobathymetry accurately. Where such determinations cannot be made, quantitative basin analysis becomes impossible.

CONCLUSIONS

Geohistory analysis of California basins supports two kinds of results: (1) general conclusions about clastic sequences deposited in tectonically active basins along complex transform systems; and (2) specific postulates about trends in the Tertiary tectonic evolution of the California continental margin.

Three general conclusions are indicated. First, sedimentation rates tended to remain roughly constant, regardless of changes in paleobathymetry, as long as the overall tectonic setting of a basin remained essentially the same (e.g., Figs. 1-5, 1-6, and 1-8). Even where rates of sediment accumulation evolved gradually or fluctuated smoothly (e.g., Figs. 1-9, 1-10, and 1-12), such variations were much less abrupt than changes in paleobathymetry. We infer that rates of delivery of clastic sediment to local basins were controlled mainly by rates of sediment production in nearby provenance terranes. As these rates of sediment production were governed chiefly by the size and relief of the provenance blocks, and by the prevailing regional climate, they were not sensitive to local paleobathymetric relations.

Second, slopes of inferred cumulative subsidence curves in tectonically active basins depend critically upon estimates of paleobathymetry (e.g., Figs. 1-4 to 1-12). Consequently, patterns of subsidence for times during which water was deep cannot be established reliably without valid paleoecological interpretations. In future work, every effort should be made to better quantify estimates of paleobathymetry, with the vagaries of restricted basins and other complicating factors taken into account. No amount of rigor in decompaction or backstripping calculations, and no amount of sophistication in flexural or thermotectonic modelling, could possibly compensate for fundamental mistakes in paleobathymetry. Parenthetically, we note that estimates of changes in the elevation of the ground surface through time are equally critical for the analysis of nonmarine basins in tectonically active regions.

Third, different procedures for decompaction produce only minor variations in inferred subsidence curves. Compared to potential errors in dating stratigraphic horizons or in estimating paleobathymetry, potential mistakes in decompaction are comparatively insignificant. The same is probably true generally for most basins containing thick clastic sequences deposited partly in deep water.

The data also suggest five postulates about the regional tectonic history of Tertiary basins in California:

1. During the Laramide interval of shallow slab descent beneath the Cordillera in latest Mesozoic and earliest Cenozoic time, insertion of a buoyant slab of oceanic lithosphere into the coastal subduction zone may have been responsible for regional uplift of the forearc region (e.g., Figs. 1-5 and 1-12).
2. Paleogene subsidence that was initiated in various local basins between mid-Paleocene and Early Eocene may have been triggered by crustal thinning associated with transtensional deformation related to dextral shear along the proto-San Andreas system (e.g., Figs. 1-6 to 1-12).
3. Uplift of various local basin floors in Late Eocene to Early Oligocene time may have been induced by subduction of buoyant young oceanic lithosphere on the eastern flank of the approaching Pacific-Farallon spreading ridge prior to initiation of the San Andreas trransform system (e.g., Figs. 1-8 to 1-12).
4. Pulses of abrupt mid-Tertiary subsidence in various local basins during Late Oligocene and Early Miocene time may have been triggered by transtensional deformation associated with initiation of the San Andreas transform system along the coastal region (e.g., Figs. 1-4 and 1-7 to 1-12).
5. Mid-Miocene and younger episodes of downwarping and upwarping in various local basins may have been produced by transpressive deformation and associated flexural effects related to wrench tectonics along the complex San Andreas transform system (e.g., Figs. 1-6 to 1-12).

ACKNOWLEDGMENTS

This study was coordinated by the senior author (WRD), who prepared the draft manuscript from a file of topical reports written by co-authors. Calculations were performed with the aid of a computer program refined by the second author (RAA), with the help of D. M. Nagi, from a prototype developed originally by Larry Mayer. Mayer earlier performed a geohistory analysis for the Los Angeles basin (see Mayer, this volume), which is not treated here. Our efforts were encouraged by knowledge of unpublished geohistory plots prepared in the past for certain California basins by T. E. Jordan and Brewster Baldwin. All figures were drafted by Rick Brokaw. Our work was supported by the Laboratory of Geotectonics in the Department of Geosciences at the University of Arizona.